

Physics Based Prognostic Health Management for Thermal Barrier Coating System

Amar Kumar¹, Bhavaye Saxena², Alka Srivastava¹, Alok Goel³

¹Tecsis Corporation, 210 Colonnade Road, Ottawa, ON, K2E 7L5
amar, alka@tecsis.ca

²University of Ottawa, 800 King Edward Street, Ottawa, ON, K1N 6N5
bsaxe011@uottawa.ca

³OMTEC Inc., 170 Bristol Road East, Mississauga, ON, L4Z 3V3
goals@sympatico.ca

ABSTRACT

Reliable prognostic of thermal barrier coating systems (TBCs) as applied to hot section engine components is a challenging task. Physics based approach is made here involving both experimental physical damage signature analysis and thermal cycle simulations. Thermally grown oxides (TGO) and the developing cracks in TBCs increase with thermal exposures. An exponential relationship is observed between the two parameters. Significant variations in size and characteristics of the damage signatures are observed depending on the four typical cycle profiles considered. In this paper, fourth order Runge-Kutta method is used for the numerical analysis of the differential equation for TGO growth analysis. Damage tolerance approach considering fracture mechanics based stress intensity factor is used to determine the crack tolerance level and remaining useful life. Our earlier fracture mechanical model for composite TBCs is modified assuming the crack to nucleate and grow within the TBC and not inside TGO. An overview of the PHM solution is presented.

1. INTRODUCTION

Combined effects of high temperature and operational stress causes accelerated damage of monolithic hot-section

* This is an open-access article distributed under the terms of the Creative Commons Attribution 3.0 United States License, which permits unrestricted use, distribution, and reproduction in any medium, provided the original author and source are credited.

parts in aeroengine and drastically shortens the useful life as compared to the life of cold section components (Chin, 2005). Common metallurgical failure mechanisms of the monolithic alloys include low and high cycle fatigue, creep/rupture, oxidation, foreign object damage and corrosion (Wood, 2000; Christodoulou & Larsen, 2005). Thermal barrier coating (TBC) systems are now widely used for aero-propulsion and power generation. TBCs applied to hot section monolithic parts provide thermal insulation to gas turbine and other high temperature engine components. By lowering the temperature of the metallic substrates improves the life and performance of the components subjected to creep, fatigue, environmental attack and thermal fatigue (Shillington & Clarke, 1999; Evans et.al., 2001). A TBC system is a two layered coating consisting of 8% yttria stabilized zirconia (YSZ), and a bond coat (BC) enriched in aluminium over a Ni base superalloy substrate. During the operation, a layer of oxidation product known as thermally grown oxide (TGO- α Al₂O₃) form and grow with time in between YSZ (top coat) and bond coat (BC) layer under the influence of mechanical and thermal stress cycles. A TBC system is truly a composite structure with TBC as the insulating top layer, TGO provides the oxidation protection, BC provides adherence of TBC on superalloy while the alloy supports the structural load. Though the current state of development of TBCs meets most of the industrial needs, yet further enhancement of stability, durability and performance of TBCs providing thermal insulation to high temperature for aero-propulsion hot-section components is the pressing industrial needs.

A great deal efforts have been made over last decade to understand the damage and failure mechanisms of TBC that

form the basis of the development of physics model, which in turn is the backbone of PHM (Shillington & Clarke, 1999; Evans et al., 2001; Kumar et al., 2007; Karlsson, Xu, & Evans, 2002; Chen et al., 2005; Clarke, Levi, & Evans, 2006). The predominant failure mechanisms for TBCs include microcrack nucleation at the TBC/BC interface layer and coalescence and propagation of cracks to cause buckling / delamination over a large part and finally to spalling. Both tensile and compressive stresses of large magnitude (up to 6 GPa) develop due to growth and thermal expansion misfit of TGO. Crack formation is facilitated by the presence of small geometric imperfections at the interface regions. Such micro/sub size defects are expected to be present / formed in coat layers due to foreign object damage, processing of coatings and thermo-mechanical operations under aggressive environments. However, none of the proposed models could explain the wide scatter in the coat life and failure mechanism of TBC system. Some of the major factors contributing to the failure and scatter in TGO life include morphology, types, oxidation rate, surface treatments, alloy and phase, bond coat roughness, TGO thickness etc. (Christodoulou & Larsen, 2005; Shillington & Clarke, 1999; Kumar et al., 2007; He, Hutchinson & Evans, 2003). A critical thickness of TGO results in critical stress to cause crack initiation inside TGO and at the interface layer.

Traditional engine health management relies on the tracking of operating hours and cycles, material properties including fatigue behavior and worst case usage data. The safe life consideration ensures component safety by limiting the probable damage that can accumulate in the material long before failure indications arise. On the other hand, prognostic health management (PHM) approach maximizes the useful life of components with enhanced safety and reliability than the conventional time based engine maintenance approach. Prognostic is the ability to assess the current condition of an engine part and predict into the future for a fixed time horizon or predict the time to failure. Continuous monitoring and analysis of engine health data and usage parameters are integrated with physics based models for diagnostic and prognostics capabilities. Other advantages of the PHM solutions are increased mission availability, minimizing maintenance and life cycle cost. A good number of commercial diagnostic PHM (DPHM) systems are now available for industrial usage and being deployed for structural health monitoring and life assessment (Intellistart⁺, Altair avionics/Pratt & Whitney, SignalProTM, Impact technologies, NormNetPHM, Frontier Technology). While the technology is nearing maturization, still the products lack in certain aspects. Major limitations include accuracy in diagnostic outcome, reliability by reducing false signal, specific applicability, offer no probabilistic confidence level and uncertainty.

The PHM technology developed so far are for monolithic systems and not applicable for TBCs which

degrade differently during engine cycle operation. The primary objectives of the present work are to address the development of models and methodology appropriate for the PHM solutions for TBCs. As opposed to safe life approach, a damage tolerant (DT) approach that accounts for crack growth is assumed to be more appropriate for the TBC applications. The DT method recognizes the fact that materials and manufacturing defects whatever minute in size it may be are present in components. The material must have high fracture resistance to be damage tolerant, even with growing cracks during operation. A fracture mechanistic (FM) approach employing stress intensity factor as the crack driving parameter forms the basis for DT approach.

2. TBC DAMAGE MODEL

Earlier studies have focused on the progressive structural damage in TBCs leading to failure by cracking and spallation (Shillington & Clarke, 1999; Evans et al., 2001; Chen et al., 2005; Clarke, Levi & Evans, 2006; LeMieux, 2003; Kumar et al., 2010; Kumar, 2009). Analytical, experimental and simulation studies have identified the formation and growth of TGO leads to damage in TBCs. TGO is essentially a thermodynamic and diffusion controlled phenomenon and is a function of both time and temperature. Both of these factors were varied in our simulated experiments in order to allow appreciable TGO growth and failure. Figure 1 displays the microstructures illustrating the formation and growth of the TGO layer in YSZ TBC subjected to thermal cycling. Details of simulated experiment, thermal cycling and damage quantification are reported elsewhere (Kumar et al., 2010; Kumar et al., 2009).

2.1 Damage Signatures

Two physical damage signatures, namely TGO thickness and crack size are identified for the complete characterization of the TBC failures. Between the two, however, TGO growth is considered as the primary damage and is strongly influenced by the exposed temperature cycles. Cracks develop at specific locations and geometry of TGO profile due to stress and strain environments and are considered as the secondary damage source. The cracking and interface separation mechanisms are influenced by shape and curvatures at the TGO boundaries as may be seen in Figure 1(b). Cracks are mostly observed at and around sharp locations and ridges as at these locations, stresses must be higher and deformability may be less compatible between the adjacent phases with growing TGO (Kumar et al., 2010; Kumar et al., 2009).The

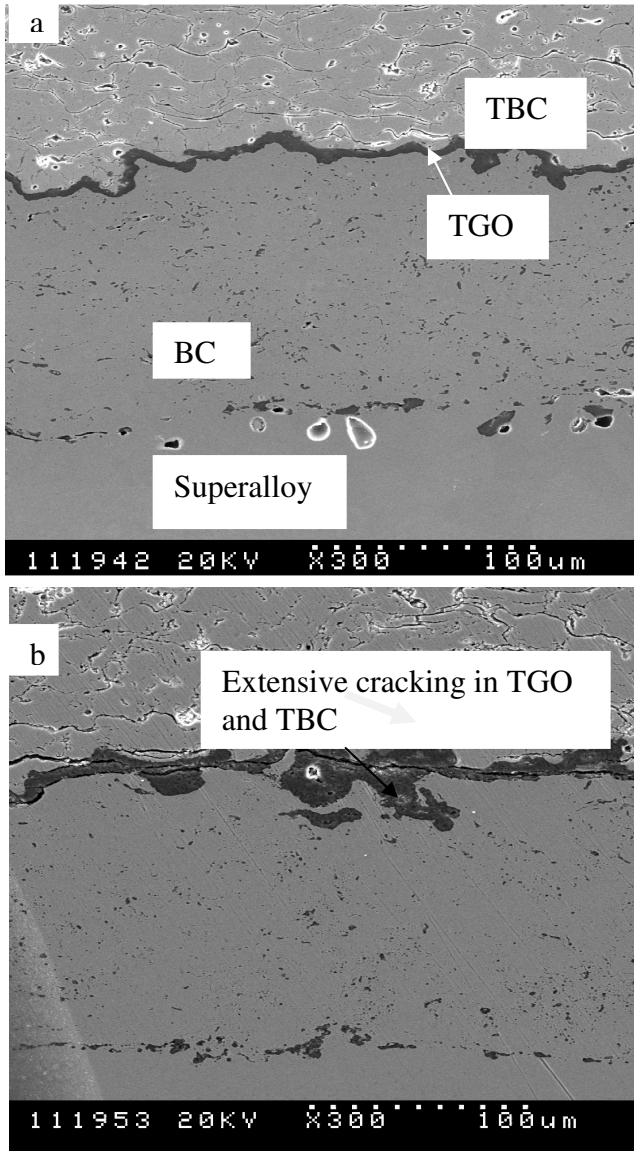


Figure 1: Microstructural demonstration of structural damages and progressive degradation in TBC; a) after 400 thermal cycles and b) after failure (around 1500 cycles).

zigzag profile of the BC-YSZ interface is held responsible for stress concentration to cause cracking at the interface and in YSZ. Experimental details for observations and quantification of damage signatures are documented elsewhere (Kumar et. al., 2010; Kumar et. al., 2009).

2.2 TGO-Crack Growth Relation

A functional relationship between the two forms of physical damages, namely crack damage and TGO growth is shown in Figure 2. Clearly and consistently, an exponential dependency between statistical mean of crack size in

different samples and the mean TGO thickness data is evident. The two plots for samples M07 (treated in normal atmospheric condition) and M08 (treated in vacuum) lie fairly close to each other demonstrating no significant effects of oxygen pressure on the physical damage size in TBC system as mentioned in earlier section. A linear relation between equivalent TGO thickness and maximum crack length was reported earlier for same TBC system (Chen et. al., 2006). An alternative and more meaningful dependency between the two parameters may also emerge by considering the first three points for both the classes having a linear function. The fourth data obtained at failures appears to follow exponentially function. This trend suggests two stage TGO growths kinetic from early oxidation until the failure time. During early stage of TBC life (up to 430 cycles), the cracking mechanisms in TBC is predominantly crack nucleation and opening controlled, while the mechanisms changes to predominant propagation controlled mode towards the later stage (exceeding 430 cycles) and until TBC failure. Two stage kinetics of oxide growth- cracking relation can be related to the changes in oxide phase changes. Alumina formation changes to mixed oxide formation consisting of Cr, Ni, Co, Al due to depletion in aluminium. Growth rate for mixed oxide is higher than alumina (Carlsson, 2007). It is confirmed that thermal cycling up to 500 cycles TGO is made of pure alumina while the internal oxide in BC consists of both alumina and spinels. However, some uncertainties are reported to be always involved in the oxide scale measurements because of higher instability of spinels as compared to alumina.

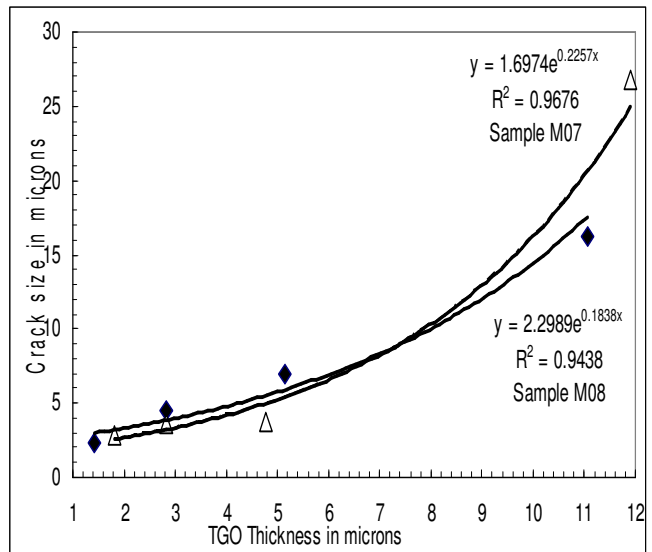


Figure 2: Exponential relationships are evident between two forms of physical damage signatures associated with thermal cycling of TBC; M07 samples were heattreated in normal air and M08 samples were heattreated in low pressure oxygen.

3. DAMAGE TOLERANCE MODEL

A damage tolerance model considering fracture mechanical approach was developed earlier for conventional three layer TBC system (Kumar et. al, 2007). The model establishes relation among various fracture critical factors, namely crack driving force, applied stress, crack size, and layer dimensions. The model considers isostrain behavior of the layers in TBC system based on the balance of elastic energy between the externally applied force and the localized stress fields around the cracks. The normalized stress intensity factor (SIF), K_I/K_0 is found to be an effective parameter in evaluating the fracture resistance of the interfaces in TBCs. The SIF ratio is represented as

$$\begin{aligned} \frac{K_I}{K_0} &= 1/\left[(m^2 - n^2)^{1/2} + \left(\frac{E_2}{E_1}\right)(1 - n^2)^{1/2} - \left(\frac{E_2}{E_1}\right)(m^2 - n^2)^{1/2} \right] \\ &= 1/\left[\left(1 - \frac{E_2}{E_1}\right)(m^2 - n^2)^{1/2} + \left(\frac{E_2}{E_1}\right)(1 - n^2)^{1/2} \right] \end{aligned} \quad (1)$$

where m is the crack depth to width ratio and n is the ratio of two adjacent layer widths. For the interface between TBC layer and TGO layer, n should be considered as the ratio of W_1 to W and for the other interface i.e. between TGO layer and BC, n should be ratio between W_2 to W (layer width W ,s are defined in Figure 3). E_1 and E_2 are the elastic moduli. Eq. (1) has been used to compute the normalized SIF for various situations that can be exploited for redesigning BC-TBC interface by FGM optimization. The damage signature data and the damage tolerance models are further exploited for prognostic health management solution for the thermal barrier coating applications. Various thermal cycles are designed and simulated to find PHM solutions as discussed in the following sections. DT model ensures that the stress intensity factor at the crack tip for a growing crack must be sufficiently smaller than the fracture toughness values for the material and loading conditions i.e. $K_{I,applied} \ll K_{IC}$. The ratio between the two K_I values gives a measure of safety factor against the linear elastic controlled fracture. However, on-line crack size measurement during thermal cycling of gas turbine blades and vanes are not simple and accurate. An indirect method based on physical damage developed in TBC for estimation of crack growth is considered.

3.1 Modification of DT Model

In the original model, the developing crack was assumed to be occurring within the TGO layer under thermal cycling. However, it is clear that the crack can grow significantly larger than the corresponding TGO thickness, especially at the later stages. This situation is illustrated in Figure 1. In order to keep the value of the Stress Intensity a real one, the crack size (a) cannot exceed the TGO thickness or the total width of the adjacent layers. If it does exceed, the value of the SIF simply becomes a complex number, and

cannot be used to represent a physical quantity in space. It is now assumed that cracks are present in the TBC layer, hence the Stress Intensity Factor is derived only for the TBC/TGO interface. The composite layer arrangement in TBCs is schematically represented in Figure 3. Details of assumptions, derivations and model are given in an earlier paper (Kumar et. al., 2007).

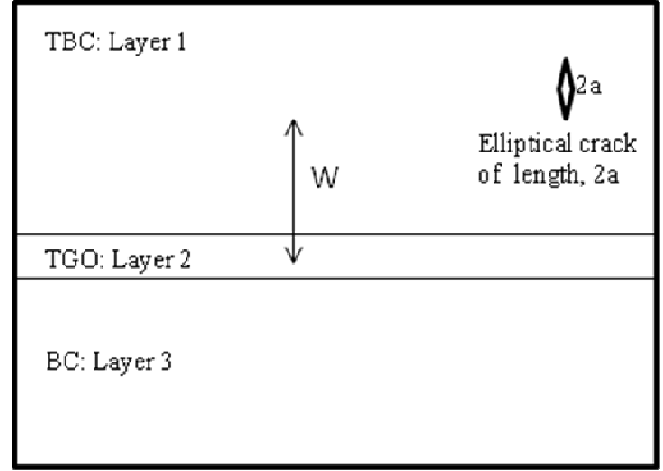


Figure 3: Cross-sectional view of the three layer layout in TBC system used for the model analysis. A thorough crack of size $2a$ is shown in the TBC layer and subjected to transverse stress, σ . Typical layer thicknesses are 300 microns for TBC ($2W_1$), 150 microns for BC ($2W_2$) and up to 15 microns for TGO layers ($2W_3$).

Westergaard's stress function and applied stress are assumed to be same as in the original model (Anderson, 1995). E_1 and E_2 are the elastic modulus of the adjacent and respective layers as in Figure 3.

$$\frac{F}{\sigma_2} = I = \int_a^{W_1} \frac{x}{(x^2 - a^2)^{1/2}} dx + \frac{E_2}{E_1} \int_{W_1}^{W_1+W_2} \frac{x}{(x^2 - a^2)^{1/2}} dx \quad (2)$$

Where E_1 (=40GPa) and E_2 (=380GPa) are the elastic modulus respectively for TBC and TGO.

$$I = (W_1^2 - a^2)^{1/2} + \frac{E_2}{E_1} \left[((W_1 + W_2)^2 - a^2)^{1/2} - (W_1^2 - a^2)^{1/2} \right] \quad (3)$$

Hence, the SIF is as follows:

$$K_I = \frac{1.12(\sigma_{applied} x (W_2 + W_1)(\pi a)^{1/2})}{I} \quad (4)$$

$$K_I = \frac{1.12 \left(\sigma_{\text{applied}} x (W_2 + W_1) (\pi a)^{1/2} \right)}{\left[(W_1^2 - a^2)^{1/2} + \frac{E_2}{E_1} \left[((W_1 + W_2)^2 - a^2)^{1/2} - (W_1^2 - a^2)^{1/2} \right] \right]} \quad (5)$$

W_1 represents the thickness of the TBC layer, which we assume remains constant throughout the evolution of the system with respect to time. Hence by dividing the numerator and denominator of Eq.(5) by W_1 , the following expression is obtained.

$$K_I = \frac{1.12 \left(\sigma_{\text{applied}} x W_1^{3/2} (1+m) (\pi n)^{1/2} \right)}{\left[(1-n^2)^{1/2} + \frac{E_2}{E_1} \left[((1+m)^2 - n^2)^{1/2} - (1-n^2)^{1/2} \right] \right]} \quad (6)$$

$$K_I = \frac{1.12 \left(\sigma_{\text{applied}} x W_1^{3/2} (1+m) (\pi n)^{1/2} \right)}{\left[\left(1 - \frac{E_2}{E_1} \right) (1-n^2)^{1/2} + ((1+m)^2 - n^2)^{1/2} \right]} \quad (7)$$

Where $n = a/W_1$ and $m = W_2/W_1$

Defining a new parameter, K_0 ,

$$K_0 = 1.12 \cdot \sigma_{\text{applied}} \cdot W_1^{3/2} \quad (8)$$

Hence, the normalized SIF can be represented as:

$$\frac{K_I}{K_0} = \frac{(1+m) (\pi n)^{1/2}}{\left[\left(1 - \frac{E_2}{E_1} \right) (1-n^2)^{1/2} + \frac{E_2}{E_1} \left((1+m)^2 - n^2 \right)^{1/2} \right]} \quad (9)$$

Hence, using Eq.(9), the result will always be a real number for the SIF determination since $(1+m)$ will always be greater than n for all real values of m and n , and n will always be less than one (assuming that the crack size is always less than the thickness to the TBC layer for realistic TBC life).

4. SIMULATION

This section describes the simulation work with temperature profile and estimation of RUL (remaining useful life). The objective of the simulation work is to make predictions of TGO as well as crack growth in the TBC system under various thermal cycles that the TBCs are likely

to be exposed. The TGO growth as mentioned earlier is strongly related to temperature (T). The TGO growth predicted with time will yield the crack size and this will be used to compute normalized SIF as shown in Eq. (9). The temperature data is required to be monitored continuously as the hot-section structural parts with TBC are operational.

4.1 TGO Estimation

The differential equation that describes the growth of the TGO layer is represented as (Mao et. al., 2006):

$$\frac{dh}{dt} = \gamma_1 \cdot 10^{\left(\frac{a_0}{T(t)} + b_0 \right) \gamma_1} \cdot h^{\left(1 - \frac{1}{\gamma_1} \right)} \quad (10)$$

Where h is the TGO thickness; $T(t)$ is the temperature profile as a function of time, t ; a_0 , b_0 and γ_0 are the fitting constants. Eq. (10) can only be solved if the temperature function is defined properly. Even if the function is known, there is not a guarantee that an integration method exists for the equation. Clearly, for time-varying temperature functions, we see that numerical analysis is to be applied. To obtain the best practical compromise between accuracy and the computational effort of the numerical analysis, the fourth order Runge-Kutta method is used.

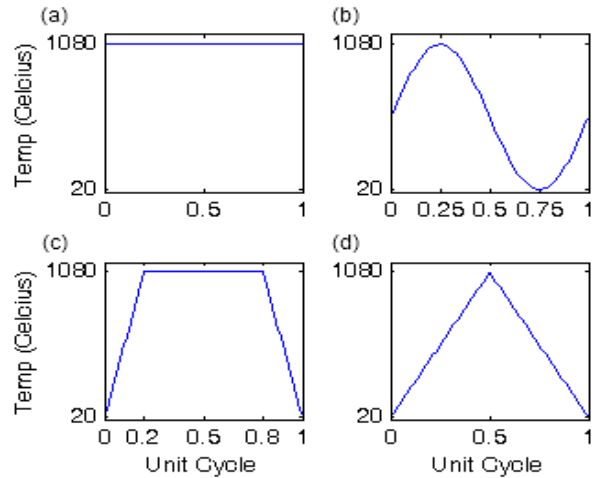


Figure 4: Schematic illustrations of four thermal cycles considered for simulation studies and experimental work. The functional relationship for each is also given. a) Isothermal case; $T(t) = 1080^\circ C$; b) Sinusoidal case; c) Trapezoidal cycle and d) Triangular cycle

To solve the generalized problem numerically, we have

$$\frac{dh}{dt} = f(h, t); h(0) = h_0; \quad (11)$$

$h(0)$ represent the initial value of the thickness h at time $t=0$. The time of interest is split into smaller intervals of duration which is written as: Δt . Thus, the time t now becomes:

$$t = n\Delta t; \forall n : 1, 2, 3, \dots, N; \quad (12)$$

Hence, the Runge-Kutta Method is known as the following iterative method:

$$k_1 = \Delta t f(h_n, n\Delta t); \quad (13)$$

$$k_2 = \Delta t f\left(h_n + \frac{k_1}{2}, \left(n + \frac{1}{2}\right)\Delta t\right); \quad (14)$$

$$k_3 = \Delta t f\left(h_n + \frac{k_2}{2}, \left(n + \frac{1}{2}\right)\Delta t\right); \quad (15)$$

$$k_4 = \Delta t f(h_n + k_2, (n+1)\Delta t); \quad (16)$$

$$h_{n+1} = h_n + \frac{1}{6}(k_1 + 2k_2 + 2k_3 + k_4) + O(\Delta t)^5 \quad (17)$$

$O(\Delta t)^5$ represents the error in the numerical method which is of fifth order with respect to the time step taken.

Four different thermal cycles are considered for simulation studies for prognostics and these are schematically displayed in Figure 4. During the flight operation the hot section parts with TBC are likely to be exposed to different thermal cycles. The maximum and minimum temperatures in all cases are maintained between 1080°C and 20°C respectively. The temperature cycle that was used in our simulated experimental research was trapezoidal temperature profile as shown in Figure 4c and functionally can be represented by the following periodic equations.

$$T(t) = \begin{cases} 1060(t)/0.2 + 20; & \text{for } 0 \leq t \leq 0.2\tau \\ 1080; & \text{for } 0.2\tau \leq t < 0.8\tau \text{ and} \\ -1060(t-0.8) / 0.2 + 20; & \text{for } 0.8\tau \leq t < \tau \end{cases}$$

$T(t)$ = Temperature at time t (°C)

τ = Duration of one cycle (=1 hr.)

Distinctly, the extent of thermal exposure of TBCs will vary with thermal cycles (Figure 4) and influence TGO growth and cracking. A comparison between the empirical relations and the actual experimental TGO growth is made in Figure 5.

There is no significant difference in the derived values and the experimentally observed data. Also, time period of the thermal cycling is negligible compared to the evolution of the TGO thickness for this case to a certain degree. The periodic equation is sufficient enough for the purpose of approximating the rise of the TGO thickness with respect to time under thermal stress. The empirical

formula can now be used to determine the TGO growth with respect to time, and eventually the values can be used for crack growth estimation as discussed in section 4.2.

4.2 Crack Growth and SIF

Till date, determining the crack size within the system has been quite a challenge. In order to predict a crack in a system, one initially needs to acquire the amount of thermal stress and the mechanical stress that will be induced to the TBC system. The process of measuring the amount of stress in the system or predicting it through the use of an algorithm has not yet been feasible, hence making it difficult for us to determine the crack size with relation to stress. This issue can be resolved by assuming a relation with respect to another variable. Since the TGO growth is the only other variable available from this experiment, a comparison between the TGO and crack size at their corresponding thermal cycle duration was conducted. The results are shown in the following section. Discussion on experimental details and quantitative estimation of damage signatures like crack size and TGO growth is beyond the scope of discussion here. Damage data was obtained by thermal cycling of TBC samples, metallography, scanning microscopy, rigorous measurements and analysis (Kumar et. al., 2010; Kumar et. al, 2009). Both Figures 2 and 5 demonstrate the relationship is of exponential type and not linear.

The relation between the thickness of the TGO and the Crack size for different number of thermal cycles appears to be exponential. The following equation for the growth of the crack size, a_c is obtained from experimental data as shown in Figure 2.

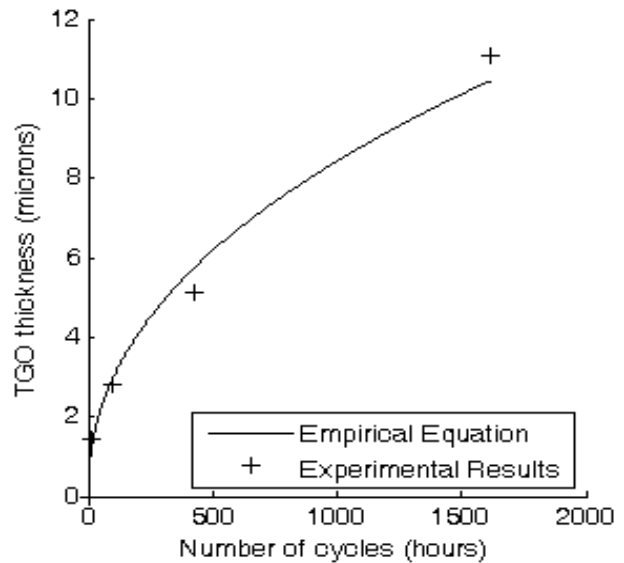


Figure 5: Comparison of simulated TGO growth in TBC with experimental data for identical thermal cycles.

$$a_t = (1.7 - 2.3) \exp(0.20 * TGO_t) \quad (18)$$

The function TGO_t is the value of the TGO thickness that will be determined from the eqs (1) to (5) which are mentioned in the previous section. As the crack size becomes available, Eq. 9 will yield the stress intensity factor as a function of time, t while the other layer dimensions and material data remaining constant.

5. PHM SOLUTION

An overview of the PHM solution for TBCs is shown in Figure 6 describing the algorithm implemented into the MATLAB™ program. The program is designed to determine the TGO thickness, crack Size, normalized SIF in real-time, trend analysis for RUL and plot new results after each calculation. A crack tolerance limit for TBCs is set in the program to allow maximum SIF that the system is supposed to withstand. In case the values overpass the margin, the plotting will carry on, but a warning sign will be indicated to the user.

computations.

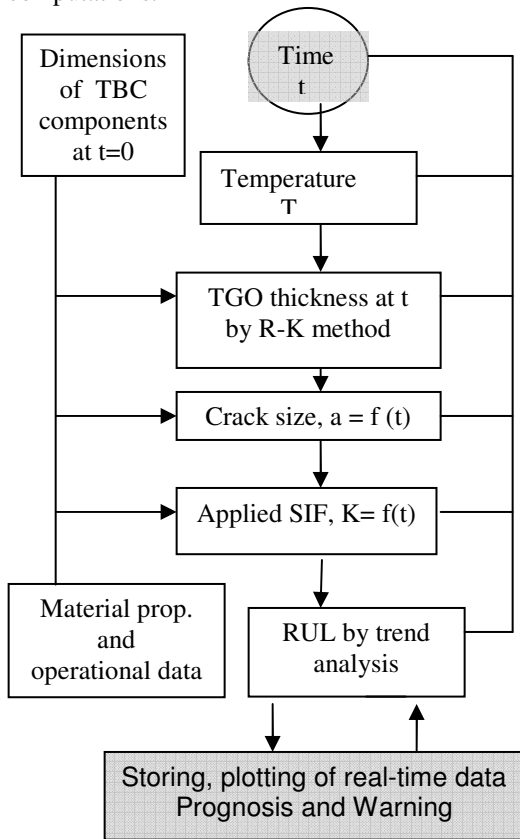


Figure 6: Overview of the proposed physics based PHM for the thermal barrier coating system as applied to hot-section components in aeroengine

As the temperature of the TBC system is measured, the timer activates the program. The TGO thickness and the crack size are determined. Now, using the TGO thickness and crack size, along with some predefined parameters such as the elastic modulus, speed, pressure and the dimensions of the TBC and BC layers, the program is able to compute the normalized SIF. All these values are then stored as an array and plotted for the user. All these operations are completed within the interval of time set for the timer, so that it does not interfere with monitored data and

5.1 RUL

Proposed PHM solution aims to obtain remaining useful life (RUL) based on the current health status of TBCs. As mentioned in earlier section that the SIF provides the current crack tolerance ability at a given time and configuration. Figure 7 illustrates the RUL estimation using SIF data and least square polynomial regression analysis. With operational cycle the TGO and cracks grow and so SIF level, prior to the attainment of threshold SIF level. Nonlinear polynomial regression through data points leads to the estimated RUL. However, the RUL will continue to vary as more new SIF data points are obtained and regression coefficients are like to change significantly. Some more discussion is relevant here with regard to TBCs crack tolerance behavior.

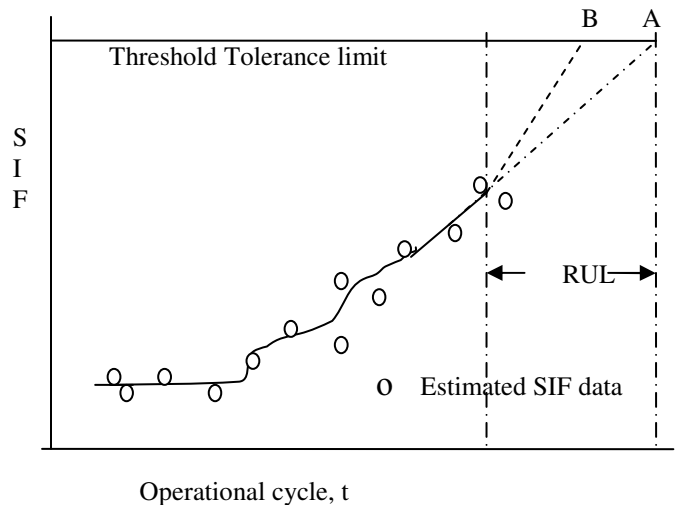


Figure 7 Illustration of RUL estimation at any point of time during operational life; points A and B signify the estimated RUL through data regression without and with some degree of conservatism.

The higher cracking and separation tendencies at TGO-TBC interface are primarily because of lower fracture resistance as compared to the BC-TGO interface. The fracture energy of the TBC-TGO interface is around only 2-4 $Mpa.m^{1/2}$ after 100 hrs. of oxidation. The fracture energy for BC-TGO layers has not been reported so far, but it is

likely to be much higher because BC layer toughness is more than $60 \text{ Mpa.m}^{1/2}$. During the early stage of growth, the separation and cracking mostly remain at and around the TGO-TBC interfaces. Under isostrain condition, an applied stress of magnitude around 100 Mpa results in K_I values of 2 to 4 $\text{Mpa.m}^{1/2}$ which is just enough for initiating a crack from a defect size of 2 microns. The stress level required for crack driving force (K_I / G_I) to be around and larger than the fracture resistance of the TBC component materials (TBC, TGO) are found to be in the range of 50 to 500 Mpa for crack size exceeding the critical length (> 1 micron) in TGO. The approximate stress levels as required for both crack initiation and propagation stages and computed from two models are consistent. The experimental work confirms the presence of cracks in the TBC system in the size range of 2-3 microns even at the onset of thermal cycling (Kumar et. al., 2010; Kumar et. al., 2009). An increasing tendency for stress intensity factor from 2 to 3.2 $\text{Mpa.m}^{1/2}$ was reported earlier with TGO growth from 4 to 8 microns (Tzimas et. al., 2000). It may be mentioned here that the research emphasized on the damage evolution and analysis for the TBC, rather than the method of prognostic analysis. However, standard regression analysis has been tried with damage signature data.

6. RESULTS

The simulation results for TGO growth and SIF estimation are given in Figures 8 and 9 for the thermal cycles considered. A smooth rise in the estimation are observed as shown in Figures 8b and 9b, while the actual pattern of TGO and SIF change can be seen at enlarger scale (up to 4 cycles) in Figures 8a and 9a respectively. Wide variations among the four are also evident in TGO, SIF and so will be in RUL as the TBC are exposed. The highest and continuous TGO growth and SIF increase are seen for isothermal temperature cycle and so the RUL may be expected to be shortest as compared to others. This is because of long uninterrupted thermal exposure at highest temperature of 1080°C. However, stepwise discontinuous changes in TGO and SIF are evident reflecting the nature of thermal cycles in other cases (Figures 4). The lowest TGO and SIF for any number of thermal cycles are obtained for triangular case as the TBCs are exposed to highest temperature momentarily. The Sinusoidal profile maintains high temperature longer than a triangular profile, thus having a faster TGO growth (Figure 8).

The other noteworthy issue affecting the RUL is that initial steep slopes of the plots tend to flatten with thermal exposure as the aluminium depletion in BC continues reducing the driving force for diffusion. The formation of other bulk mixed oxides, e.g NiO, $(\text{Cr, Al})_2\text{O}_3$, Fe_2O_3 , $(\text{Ni,CrAl})_2\text{O}_4$ etc. (Chen, Wu, Marple & Patnaik, 2005;

Chen, Wu, Marple & Patnaik, 2006; Sidhu & Prakash, 2005) also reduce the kinetics of oxidation process. Though maximum temperature has the major effect on RUL, but nature of oxidation and damage state depending upon the thermal cycle also determines the life time. Reducing the temperature from 1177°C to 1130°C is reported to increase sample lifetime by a factor of 2.4, though the damage state is observed to be same irrespective of temperature profile as long as the peak temperature remains constant (Nusier, Newas & Chaudhury, 2000).

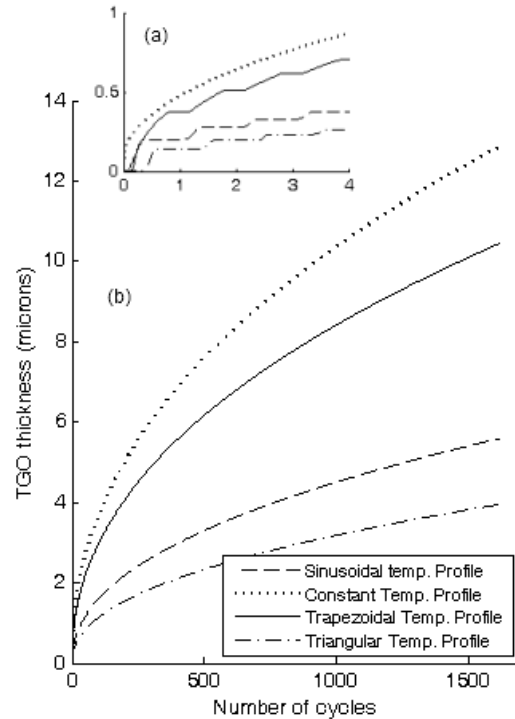


Figure 8: TGO growth rate characteristics in TBCs exposed to different thermal cycles; a) at magnified scale showing actual pattern of growth and b) at reduced scale indicating smooth rise for TGO thickness.

The other noteworthy issue affecting the RUL is that initial steep slopes of the plots tend to flatten with thermal exposure as the aluminium depletion in BC continues reducing the driving force for diffusion. The formation of other bulk mixed oxides, e.g NiO, $(\text{Cr, Al})_2\text{O}_3$, Fe_2O_3 , $(\text{Ni,CrAl})_2\text{O}_4$ etc. (Chen, Wu, Marple & Patnaik, 2005; Chen, Wu, Marple & Patnaik, 2006; Sidhu & Prakash, 2005) also reduce the kinetics of oxidation process. Though maximum temperature has the major effect on RUL, but nature of oxidation and damage state depending upon the thermal cycle also determines the life time. Reducing the temperature from 1177°C to 1130°C is reported to increase sample lifetime by a factor of 2.4, though the damage state is observed to be same irrespective of temperature profile as

long as the peak temperature remains constant (Nusier, Newas & Chaudhury, 2000). However, further experimental studies on the nature of oxidation and damage and cracking mechanisms under different thermal cycles are required to substantiate the results.

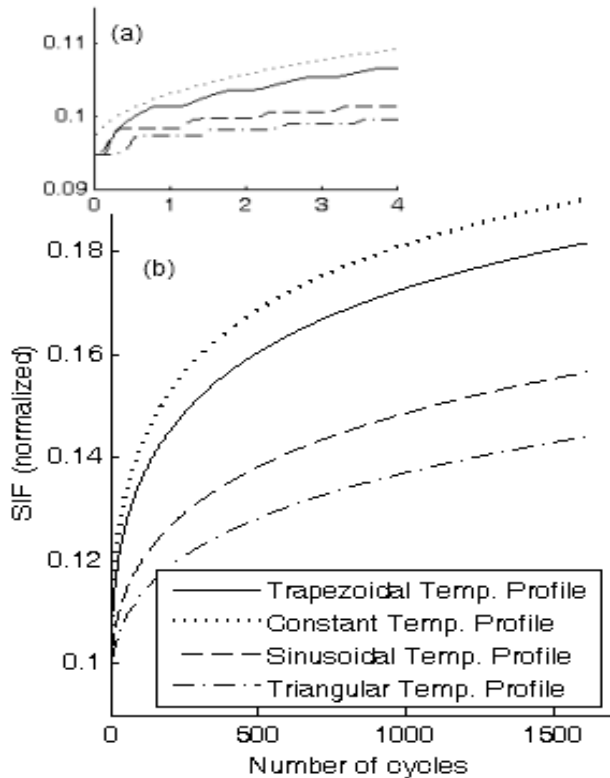


Figure 9: SIF change with number of cycles as TBCs are exposed to different thermal cycles; a) at magnified scale showing actual pattern and b) at reduced scale indicating smooth increase of SIF.

7. CONCLUSIONS

Experimental and simulation studies on the prognostic assessment of thermal barrier coating system were carried out using physics based approaches. Two damage signatures, namely growth of aluminium oxide at the interface between bond coat and top insulating coat and the cracks are responsible for the failure of TBCs. An exponential relationship between the two signatures is established. Temperature being the driving force for diffusion and TGO, four thermal cycle profiles are simulated and fourth-order Runge-Kutta method is used for numerical solution. For TBC system stability and crack tolerance, a modified fracture mechanical model is used assuming that the cracks form and grow in the top TBC layer. The normalized stress intensity factor determines the current health and remaining useful life using the regression

analysis. The TGO and crack tolerance level based on the simulation results vary widely and largely depends on the extent of thermal exposure to TBC.

ACKNOWLEDGEMENT

Authors gratefully acknowledge the generous support and encouragement received from Institute of Aerospace Research, NRC, Ottawa for conducting experiments with thermal barrier coating samples.

REFERENCES

- Chin, H. H., Turbine engine hot section prognostics, <http://www.appliedconceptresearch.com/Turbine%20Engine%20Hot%20Section%20Prognostics.pdf>
- Wood, M. I., (2000), Gas turbine hot section components: the challenge of residual life assessment, *Proceedings of Institution of Mechanical Engrs.*, 214 part A, pp. 193-201.
- Christodoulou, L. & Larsen, J. M., (2005), Material Damage Prognosis: A Revolution in Asset Management, in *Material damage Prognosis* (ed. J M Larsen et.al.), TMS, pp. 3-10.
- Intellistart⁺, Altair avionics/Pratt & Whitney; <http://www.altairavionics.com/>
- SignalProTM, Impact <http://impact.tek.com/Aerospace/Aerospace.html>
- NormNetPHM, Frontier Technology Inc., <http://www.fti/net.com/products/NormNet-prod/NormNet.html>
- Shillington, E.A.G. & Clarke, D.R., (1999), Spalling failure of a thermal barrier coating associated with aluminium in the bondcoat, *Acta Materialia*, vol. 47, 4, pp.1297-1305.
- Evans, A. G., Mumm, D. R., Hutchinson, J. W., Meier, G. H. & Pettit, F. S., (2001), Mechanisms controlling the durability of thermal barrier coatings, *Progress in Materials science*, vol.46, pp. 505-533.
- Kumar, A. N., Nayak, A., Patnaik, A. R., Wu, X. & Patnaik, P.C., (2007), Instability analysis for thermal barrier coatings by fracture mechanical modelings, *Proceedings of GT2007, ASME Turbo Expo 2007: Power for Land, Sea and Air*, GT 2007 – 27489, Montreal, QC.
- Karlsson, A. M, Xu, T. & Evans, A G., (2002), The effect of thermal barrier coating on the displacement instability in thermal barrier system, *Acta Materialia*, vol.50, pp. 1211-1218.
- Chen, W. R., Wu, X., Marple, B. R. & Patnaik, P.C., (2005), Oxidation and crack nucleation / growth in an air-plasma-sprayed thermal barrier coating with NiCrAlY bond-coat, *Surface and Coating and Technology*, vol. 197, pp. 109-115.
- Clarke, D.R., Levi, C. G. & Evans, A. G., (2006), Enhanced zirconia thermal barrier coating systems, *Journal of Power and Energy*, Proc. I. MechE, vol. 220, pp.

85- 92.

- He, M.Y., Hutchinson, J. W. & Evans, A. G.,(2003), Simulation of stresses and delamination in a plasma-sprayed thermal barrier system upon thermal cycling, *Materials science and Engineering*, vol. A345, pp. 172-178.
- LeMieux, D. H., (2003), Online thermal barrier coating monitoring for real time failure protection and life maximization, *Report US Department of Energy*, DE-FC26 -01NT41232.
- Kumar, A., Srivastava, A., Goel, N., & Nayak, A., (2010), Model based approach and algorithm for fault diagnosis and prognosis of coated gas turbine blades, *Proceeding of IEEE/ASME International conference on Advanced Intelligent Mechatronics*, Montreal, QC.
- Kumar, A., Nayak, A., Srivastava, A., & Goel, N. (2009), Experimental validation of statistical algorithm for diagnosis of damage fault, *Proceedings of IEEE Canadian conference on electrical and computer engineering*, St. John's.
- Chen, W.R., Wu, X., Marple, B.R. and Patnaik, P.C.,(2006), The growth and influence of thermally grown oxide in a thermal barrier coating, *Surface and Coating Technology*, vol. 201, pp.1074-1079.
- Carlsson, K.,(2007), *A Study of failure development in thick thermal barrier coating*. Master thesis in Mechanical Engineering, Linkopings University Tekniska Hogskolan, Sweden.
- Anderson, T. L., (1995), *Fracture Mechanics: Fundamentals and Applications*, Boca Raton, CRC Press, USA.
- Mao, W. G., Zhou, Y. C., Yang, L., & Yu, X. H. (2006), Modeling of residual stresses variation with thermal cycling in thermal barrier coatings, *Mechanics of Materials*, vol. 38, pp. 1118-1127.
- Tzimas, E., Mullejans, H., Peteves, S. D. Bressers, J. and Stamm, W.,(2000), Failure of TBC systems under cyclic thermomechanical loading, *Acta Materialia*, 48(18-19),pp. 4699-4707.
- Sidhu, B.S. & Prakash, S. (2005), High temperature oxidation behavior of NiCrAlY bond coats and stellite -6 plasma -sprayed coatings", *Oxidation of Metals*, vol. 63, 314, pp. 241-259.
- Nusier, S. Q., Newas, G. M & Chaudhury, Z. A. (2000), Experimental and analytical evaluation of damage processes in thermal barrier coatings, *International Journal of Solids and Structures*, vol. 37, 18, pp. 2495-2506.

Amar Kumar has more than 25 years of research and consulting experience in the fields of structural materials characterization and development, fracture mechanics, failure analysis and applications. At present Dr. Kumar is working as senior research scientist in the development projects of diagnostics, prognostics and health management

of aeroengine components. Prior to joining the current assignment in 2006, he was employed with Indian Institute of Technology at Delhi, India as a teaching faculty after obtaining his Ph.D degree from the same Institution. Dr. Kumar has published more than 150 research papers in refereed journals, conference proceedings, and technical reports.

Bhavaye Saxena is currently an undergraduate student in the University of Ottawa under the department of Physics. His interests lie in computational physics, and have recently put interest in deriving models related to engineering physics.

Alka Srivastava has 24 years of research, administrative and industrial experience and has a BAsC degree in Electrical engineering from University of Ottawa. At present she is the manager of the R & D Division and leads several teams working in the fields of Fault Tolerance, Prognostic health management etc.

Alok Goel has more than 30 years of manufacturing, research, and industrial experience. He has a M.Sc degree in Advance Manufacturing Systems & Technology from University of Liverpool, UK. At present he is President of OMTEC Inc., (Consulting Engineer's). His research interests are in naval fuel filtration and lube oil separation. He is specialized in manufacturing graded natural fiber as a filler material for plastic reinforcement application.